ROTORCRAFT FUSELAGE WEIGHT ASSESSMENT IN EARLY DESIGN STAGES

D. B. Schwinn[1)], P. Weiand[2)], M. Buchwald[2)], M. Schmid[3)]

German Aerospace Center (DLR)
[1)] Institute of Structures and Design, Pfaffenwaldring 38-40, 70569 Stuttgart
[2)] Institute of Flight Systems, Lilienthalplatz 7, 38108 Braunschweig
[3)] Institute of Aerodynamics and Flow Technology, Lilienthalplatz 7, 38108 Braunschweig

Abstract

Like the design of fixed-wing aircraft the design of rotorcraft is generally divided into the three consecutive phases of conceptual, preliminary and detailed design. During each phase the acquired results in turn serve as input for new calculations, thus increasing the detail level and information about the new concept while uncertainties about the new design are reduced. An important aspect of the overall design process is the weight estimation in early design stages. The weight of the rotorcraft drives the design of many important components, such as the rotor(s), the propulsion system and, therefore, the required fuel. The fuselage is considered as the central structural part since it connects all other components to each other and serves as protection of the occupants but in the past it often turned out to also be the heaviest part of all rotorcraft components. This paper shows an approach to estimate rotorcraft component weights using statistical methods based on existing rotorcraft but also an approach to use finite element methods that determine the structural airframe weight based on mission profiles respectively bearable load cases.

Keywords

Rotorcraft design; weight estimation; structural analysis; conceptual and preliminary design; fuselage sizing

Symbols

f	surface correction factor
f_{ramp}	factor to consider cargo ramp installation
h	height
L	tool level
l	length
l_{fus}	fuselage length
m_{em}	(basic) empty mass
m_{fe}	furnishings and equipment group mass
m_{fuel}	fuel mass
m_{fus}	fuselage mass
m_{mto}	maximum take-off mass
m_{oem}	operating empty mass
m_{oi}	operator items mass
m_{pay}	payload
m_{prop}	propulsion group mass
m_{struct}	structural group mass
m_{sys}	systems group mass
n_i	number of interfaces
n_t	number of design tools
n_z	design ultimate load factor
s_f	scaling factor
t	thickness
s_b	body surface
w	width
W_e	empty weight
W_g	design gross weight
σ_{eqv}	equivalent stress
χ	technology factor for weight scaling

Abbrevations

AFDD	U.S. Army Aeroflightdynamics Directorate
APDL	ANSYS Parametric Design Language
COG	center of gravity
CPACS	Common Parametric Aircraft Configuration Schema
DFEM	detailed FEM
DLR	German Aerospace Center (Deutsches Zentrum für Luft- und Raumfahrt)
EDEN	Evaluation and Design of Novel Rotorcraft Concepts
FE	Finite Elements
FEM	Finite Element Method
FSD	fully stressed design
GFEM	global FEM
HOST	Helicopter Overall Simulation Tool
IRIS	Integrated Rotorcraft Initial Sizing
PANDORA	Parametric Numerical Design and Optimization Routines for Aircraft
RCE	Remote Component Environment
RIDE	Rotorcraft Integrated Design and Evaluation
SAWE	Society of Allied Weight Engineers
TIGL	TIVA Geometric Library
TIVA	Technology Integration for the Virtual Aircraft
TIXI	TIVA XML Interface
TLAR	Top Level Aircraft Requirement
TRIAD	Technologies in Integrated and Advanced Design
UTH	Utility/transport helicopter
xml	extensive markup language

1. INTRODUCTION

Designing a new rotorcraft is a complex challenge. Like fixed-wing aircraft it involves different disciplines. In order to get the optimum design, the multiple disciplines have to interact right from the start.

In general, aircraft design is separated into three classical stages, for instance as given by Raymer [1]: the conceptual phase, the preliminary phase, and the detailed design phase.

The conceptual design is mainly driven by the attempt to determine the external configuration that fulfills the top level aircraft requirements (TLARs). Typical (and frequently used) TLARs are for instance range, payload, cruise speed, or cabin volume. The generation of a concept study already involves several disciplines. To assess different concepts the design engineers need fast analysis methods due to the high amount of analyses to be conducted. Therefore, the tools used in the conceptual design phase feature many simplifications. Generally, the conceptual design stage can be considered as finished when the major design parameters have been established, such as the generation of an outer aerodynamic surface, often referred to as loft (exemplary see Fig. 1).

The preliminary design uses higher fidelity tools to account for an increasing detail level. In this design stage a basic internal arrangement is elaborated. Structurally seen, the aforementioned outer configuration is provided with primary structure, such as frames, stringers, and fuselage skin panels. The distribution of the primary structure follows knowledge based engineering rules. Typical requirements are the reinforcement of fuselage cutouts in order to bypass the loads around openings, such as doors. Other requirements arise due to the positioning of the main rotor which requires a reinforced mounting to the airframe. The possible design solutions in this phase follow a much narrower path than in the conceptual design phase. Due to the information gained in the conceptual design stage there is more input available for the calculations but there is also both, more and more detailed output, so that the tools in this design phase often require more computational power and processing times.

The detailed design phase deals with detailed solutions, often driven by manufacturability reasons. The tools used in this stage feature the highest demand of computational resources, labor time, and manpower.

A fundamental part of the design process is the weight – or mass - estimation. In the conceptual design stage the weight estimation is required to define and assess the required flight performance of the novel rotorcraft. In the preliminary design stage the ground and flight loads, which result from the estimated weight, are the basis for the structural sizing which in turn influences the weight and therefore the flight performance. In this phase the term *weight estimation* turns into the term *weight assessment* since the results are not purely based on statistics anymore, therefore, the deviation from the true weight is expected to decrease. In the detailed design phase the weight estimation can be considered as a constraint since any additional weight penalties, caused by constructional requirements, may negatively influence the weight and thus, the desired flight performance.

The fuselage represents an important part of the rotorcraft. It serves as a central mounting for all parts and as an aerodynamic shielding for the occupants. Consequently it often represents the heaviest component of the overall rotorcraft. Therefore, the fuselage features high weight saving potential and deserves a more detailed examination.

In 2010, the German Aerospace Center (DLR) started with the generation of an automated and integrated design environment for rotorcraft in order to assess novel rotorcraft configurations addressing typical rotorcraft limitations, such as speed or noise. During the projects RIDE (Rotorcraft Integrated Design and Evaluation) and EDEN (Evaluation and Design of Novel Rotorcraft Concepts) the data format CPACS (Common Parametric Aircraft Configuration Schema, [2]) was adapted to match parametric rotorcraft description. The network based simulation environment RCE (Remote Component Environment, [3]) was used to set up the workflows for the design processes of generic rotorcraft. Within the DLR internal project TRIAD (Technologies for Rotorcraft in Integrated and Advanced Design), which started in 2018, the tools developed in the preceding projects were integrated into the new design environment IRIS (Integrated Rotorcraft Initial Sizing). The tools used in this environment cover the phases of conceptual, and partly the preliminary design.

This paper describes the weight estimation processes in the conceptual design stage established within the aforementioned projects. Moreover, it shows an approach to assess the fuselage weight in the preliminary design stage.

2. DESIGN ENVIRONMENT

One of the primary features of this design environment is the use of a distributed computation. Therefore, IRIS constitutes a combination of RCE as collaboration software connecting the different servers, and the CPACS data model as a universal language between the individual tools.

Starting a highly iterative design process requires the setup of an initial configuration at the beginning. The minimum required TLARs are most commonly payload, range, maximum cruise speed, the rotorcraft configuration (standard configuration with main and tail rotor, coaxial configuration, and tandem configuration) as shown in Fig. 1, and the blade amount of the rotor(s). These parameters are specified by the customer respectively the user at the beginning of the design study. Other parameters are calculated by either statistical or physical methods during the design process.

A major aspect to handle an integrated and automated tool chain is a flawless connection and communication between all involved tools. As language to describe the rotorcraft and to control the input and output of the tools, the in-house developed CPACS data model was chosen and extended by the specific data describing rotorcraft. The additional data basically consist of the description of the rotors, which is typically not covered by fixed-wing design.

The CPACS data model serves as interface between the involved tools. In the beginning of the design process, it is an empty file that is filled with results after each analysis, thus increasing the detail level. Certain tools require input that must be computed by other tools first, therefore, the tool order must be arranged wisely.

FIGURE 1. Implemented rotorcraft configurations

CPACS is an xml (extensive markup language) based data model to describe parametric aircraft. Its benefits are its hierarchical structure, readability, and easy access. Using CPACS as integral key component for data exchange, the amount of required tool interfaces can be significantly reduced, thus increasing clarity of the calculation modules. The quantity of required tool interfaces is reduced from a quadratic approach for the traditional design structure

$$n_i = n_t(n_t - 1) \quad (1)$$

to a linear approach

$$n_i = 2n_t \quad (2)$$

with CPACS as common design language where

n_i number of required interfaces,

n_t number of design tools.

Figure 2 shows an interface scheme of the traditional approach where each tool directly communicates with any other tool (on the left) and the centralized CPACS approach (middle) while the graph on the right schematically visualizes the reduction of interfaces indicating simplified maintenance.

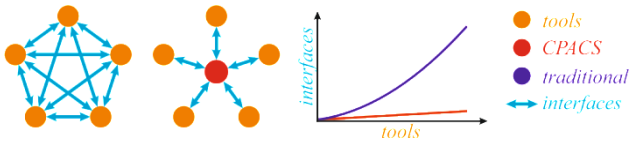

FIGURE 2. CPACS benefits

In order to efficiently work with the CPACS data model the two libraries TIXI (TIVA[1] XML Interface, [4]) and TIGL (TIVA Geometric Library, [5]) are used since they provide standardized routines to access the data within CPACS. TIXI is a library for the handling of input and output data in text format while TIGL is a graphic library that provides functions to process geometric information of the aircraft model.

To set up workflows that connect and execute the tools developed by the participating institutes the in-house software RCE was chosen: Each institute provides a server with its tools locally installed. An internal network is used to access instances of the tools that all use a specified CPACS file as input and output, respectively. Advantages of RCE are that the program code never leaves the facility where it was developed, thus the institute's knowledge remains where it was developed. Moreover, the responsible engineer can easily maintain and improve the code on site.

With respect to the computation time, the uncertainties, the robustness, and the amount of required input data the variety of design tools applies to different methods of modeling. Hence they are classified into four major fidelity categories ranging from level L0 to L3:

- L0 tools: They mostly use empirical methods with many very simple physical assumptions. They provide much output with only very limited input. A typical application is the initial sizing as depicted in Fig. 3.
- L1 tools have a better physical modeling but still are fast enough to perform iterative procedures. Therefore, they are widely used for primary sizing tasks, (see Fig. 4). This class of tools is used for the conceptual design part in IRIS.
- L2 tools feature a very good physical modeling. As a disadvantage, they require much computational power and a more detailed input to work reliable. They produce a high amount of output which cannot always be handled automatically.
- L3 tools are considered as the most complex design tools. They have the highest computational demand with regard to power and time. Moreover, their pre-processing of the computational model and the post-processing of the calculated results cannot be performed automatically. This class of tools is typically used during the detailed design phase.

The general process structure, as it is currently implemented in IRIS, is schematically illustrated in Fig. 3.

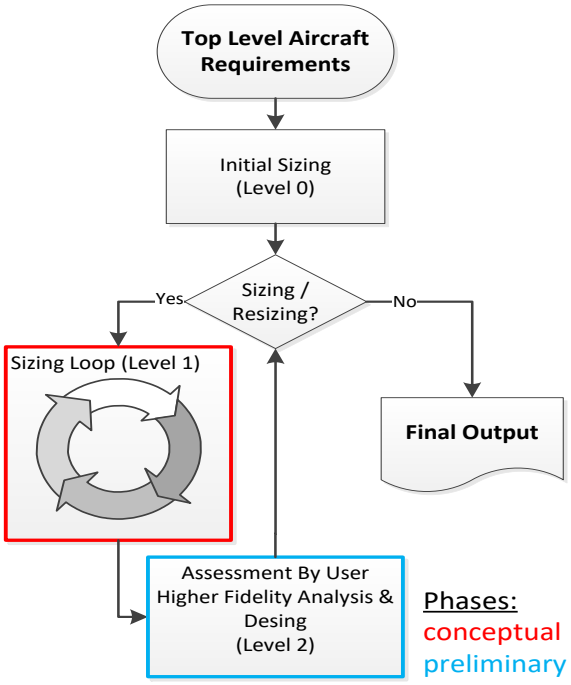

FIGURE 3. Flowchart of the virtual design approach [6]

In general, the L0 tools create the first data. The L1 tools complete the data and the L2 tools extend the data. The TLARs dictate a primary configuration with an initially estimated design gross weight respectively mass which corresponds to the maximum take-off mass m_{mto}. At this early stage of the design process it is roughly estimated by L0 tools using statistical methods. This approach impedes novel design approaches since statistical data is not sufficiently available. The sizing loop (depicted in red) is conducted using L1 tools and corresponds to the conceptual design phase. The arrangement of the L1 tools of the sizing loop from Fig. 3 is illustrated as flowchart in

[1] TIVA (Technology Integration for the Virtual Aircraft) was a DLR project from 2005 – 2009 that marks the beginning of extensive multidisciplinary collaborations at DLR [31]

more detail in Fig. 4. If m_{mto} has converged during this stage, the design process shifts to the preliminary design phase (corresponds to the blue box in Fig. 3). Higher fidelity tools are used to further optimize the configuration of the conceptual design stage. Since the computation times of L2 tools usually exceed the demanded limits of the conceptual design stage, they are used outside the sizing loop. If the results of the higher fidelity computations show major deviations between the L1 and L2 tools, technology factors must be applied in order to perform a resizing of the configuration with the L1 tools. Hence, Figure 4 shows possible input from L0 tools as well as from L2 tools as input.

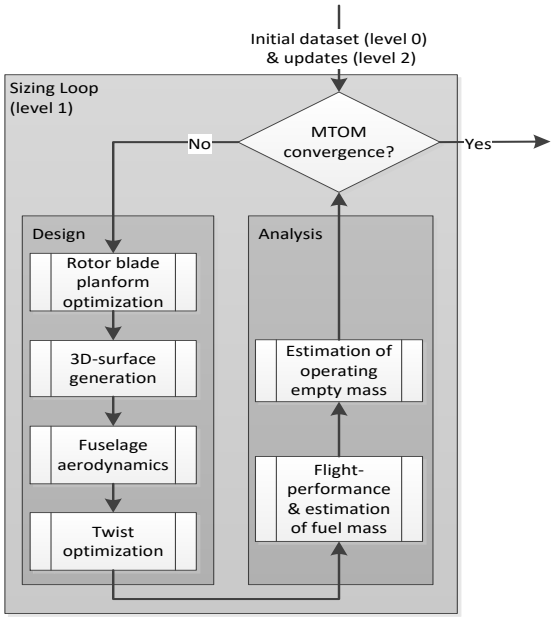

FIGURE 4. Flowchart of the L1 sizing loop [6]

In the initialization phase, an empty CPACS file is generated and a basis configuration is stored. Based on a dataset of about 160 helicopters, a first maximum take-off mass is estimated, serving as starting point for the subsequent sizing processes. During the design branch, the design of the configuration is developed to account for the TLARs respectively requirements that have been generated by previous tools. The primary and most important step in the sizing loop is the calculation of the main rotor dimensions, as its characteristics are substantial for the performance of the overall design. A knowledge based procedure [7] can be applied for the optimization of the rotor radius, blade chord, and blade tip speed.

After the sizing of the rotors, a three dimensional model of the rotorcraft is developed by sizing a generic fuselage assembly with respect to the determined component scales. The responsible tool automatically instantiates fuselage components from a catalogue and scales them to match the required overall dimensions. A three dimensional geometry model is automatically generated in CATIA and subsequently transformed into the CPACS denoted description of profiles and sections for further geometric processing, e.g. aerodynamic or structural analyses. Figure 5 shows how the fuselage is assembled by the individual components. A detailed description of the geometry generation module is given by Kunze [8].

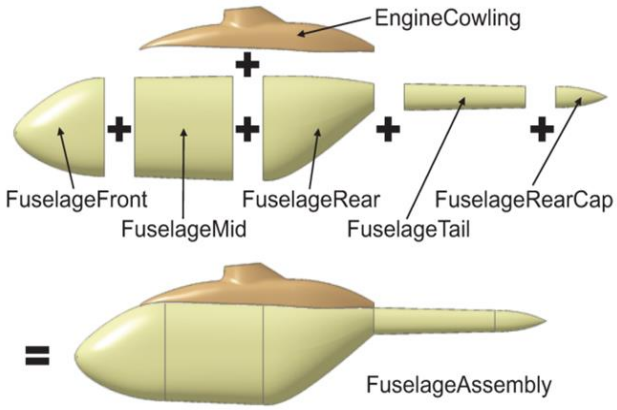

FIGURE 5. Assembly of fuselage components [8]

Subsequently, the aerodynamic properties are calculated by a module applying potential flow theory with an incompressible and inviscid approach. Corrections that consider compressibility effects can be assessed by the integrated Prandtl-Glauert or Karman-Tsien approaches. In order to take into account viscous effects and boundary layer transition and separation can be evaluated by applying an integrated boundary layer formulation. Pressure drag is estimated based on the calculated separation line. Handbook methods have been integrated to correct the obtained force coefficients in order to cover the influence of skids and additional attachments. The aerodynamic coefficients of the stabilizers are calculated separately.

An optimization of the linear part of the blade twist can be performed in order to minimize the required power for a design flight condition. The trim calculation for this procedure is conducted by the tool HOST (Helicopter Overall Simulation Tool, [9]). If this step is performed the computation of all required parameters for the flight simulation model has to be conducted earlier.

In the analysis branch the maximum take-off mass is recalculated. With the flight performance calculation the required fuel mass for the design mission is computed iteratively. HOST is used for the required trim calculations: For all flight segments, trim calculations are performed at least at the beginning and at the end of every segment to obtain the required power in order to predict the mean fuel flow and actual range. The actual and required range are compared to each other which leads to a correction of the actual fuel mass until it converges and the required range is met. A more detailed description of the flight performance analysis and the estimation of the fuel mass is given by Buchwald et al. [10] while Weiand et al. [6, 11] provide more information on the overall design process.

The component weight estimation concludes the analysis section as enough parameters have been calculated to create a mass breakdown allowing for a more precise m_{mto}. This updated maximum take-off mass then serves as input for sizing loop iterations. Convergence of m_{mto} marks the end of the conceptual design phase so that the external configuration with the derived mass breakdown and the corresponding required flight performance are available in a reasonable and consistent relation for the preliminary design stage.

The weight estimation process in general is described in more detail in ch. 3 while the statistical approaches for the

conceptual design phase implemented in IRIS are introduced in ch. 4.

3. WEIGHT ESTIMATION

Weight respectively mass estimation is a fundamental part of the overall design process. The design gross weight is considered as a central design parameter. It determines and influences many design parameters. As example, the maximum take-off weight, respectively mass m_{mto} of the helicopter determines the rotor characteristics since the rotor has to generate the necessary lift for hovering and flight. The power to drive the rotor, in turn, dictates the engine(s) which then determines the fuel amount to successfully conduct the requested missions. These components in turn influence other component weights, such as gear box, drive system, hydraulics, electrics, etc. as well as the structural weight.

The reduction of fuel weight and thus m_{mto} is a major objective in aeronautical design as it has a favorable effect on flight performance and operating expenses [12]. Estimating m_{mto} too low may lead to a comparable weak structure which might deform irreversibly (or even fail) under extreme conditions. In contrast, estimating m_{mto} too high may lead to an excessive structural weight which reduces the efficiency and increases cost. Therefore, an estimation of m_{mto} as precise and early as possible is an important and essential task during the design process.

The maximum take-off mass m_{mto} is of particular interest in the design process since it represents the heaviest configuration of an aircraft at which it has to fulfill all applied airworthiness requirements. It can be broken down into

$$m_{mto} = m_{oem} + m_{pay} + m_{fuel} \quad (3)$$

where

m_{oem} operating empty mass,

m_{pay} (required) payload,

m_{fuel} (necessary) fuel mass.

In general, the payload is a requirement specified by the customer and consists of passengers and/or cargo. The operating empty mass m_{oem} represents the empty aircraft ready to be operated. It is broken down into

$$m_{oem} = m_{oi} + m_{em} \quad (4)$$

with m_{em} representing the dry, empty mass of the rotorcraft. The so-called operator items mass m_{oi} represents the mass of items which are not necessarily required to operate the rotorcraft but are desired by the operator, such as seats, safety equipment, system fluids, cabin amenities, etc. The empty mass m_{em}, therefore, represents the empty, dry weight of the aircraft and is calculated as sum of the aircraft group masses

$$m_{em} = m_{struct} + m_{prop} + m_{sys} + m_{fe} \quad (5)$$

where

m_{struct} structural mass,

m_{prop} propulsion system mass,

m_{sys} mass of all installed systems,

m_{fe} mass of the furnishings and equipment.

The group weights represent the sum of the individual contained components. The component weight estimation within IRIS follows the standards proposed in RP 8 (Recommended Practice Number 8) [13] by the Society of Weight Engineers (SAWE).

4. STATISTICAL WEIGHT ESTIMATION

In the early conceptual design only limited data is available. Therefore, at that time of the design process, statistical approaches are used to estimate the rotorcraft mass breakdown. However, novel configurations can only be roughly estimated by comparison to already existing rotorcraft of similar configuration. In the presented design environment IRIS the methods proposed by Beltramo and Morris [14], Layton [15], Palasis [16], Prouty [17], and the AFDD (U.S. Army Aeroflightdynamics Directorate) models provided by Johnson [18] have been implemented.

Figure 6 shows a comparison of the different weight estimation methods for a generic medium-sized utility rotorcraft in standard configuration with a comparable mission profile to a Eurocopter EC135.

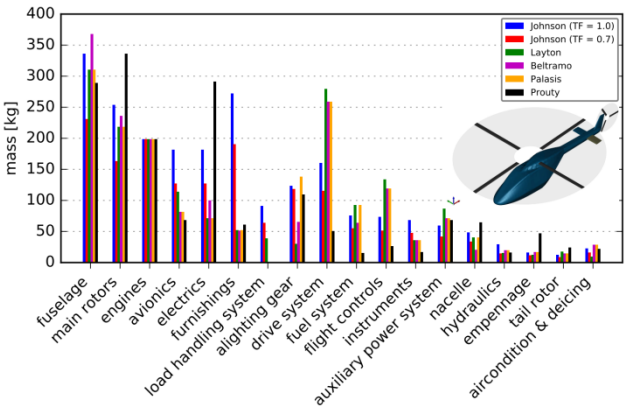

FIGURE 6. Comparison of the implemented methods

It can be observed that the methods provided by Johnson seem to estimate the highest masses when a calibration of the models by technology factors is not conducted. The estimation of the correct technology factor for each individual component is a challenge which, in general, requires sophisticated knowledge about the mass breakdown of a reference configuration. Since this type of information is very sensitive to the manufacturers, it is rarely published and therefore this circumstance complicates the estimation of the correct technology factors. However, as the maximum take-off mass of the reference configuration, including the shares of payload mass, basic empty mass, and fuel mass is known [11] it is reasonable to apply one common technology factor to all component masses. The use of an overall technology factor for all component weights smears the component weights for the sake of a correct estimation of m_{mto}. This approach was also performed by Russel and Basset [19]. A technology factor of χ=0.7 led to a deviation of about 3% of the estimated m_{mto} to the reference configuration $m_{mto,ref}$.

The mass estimation of some systems in IRIS follows an approach based on Johnson's methods: Certain systems, such as e.g. instruments or hydraulics, are estimated by linear interpolation between lower and upper limits for medium to heavy weight helicopters, as illustrated in Fig. 7. Alternatively fixed weights for these systems can be

specified. In case, a certain component weight is known (or desired) it can be stored in the corresponding CPACS node and will not be changed in subsequent iterations.

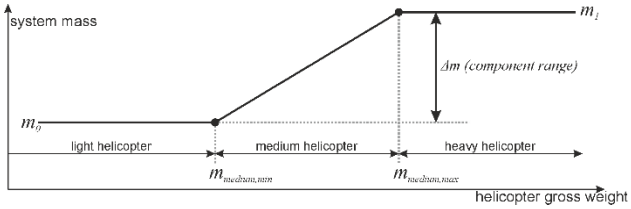

FIGURE 7. Linear interpolation of system masses

A composition of the empty mass calculated using the calibrated AFDD models (as displayed in Fig. 6) is shown in Fig. 8. It is observable that the fuselage weight constitutes the highest share. It shall be noted that this composition represents one specific, generic configuration. However, the shares of the individual components can be considered as comparably precise and, therefore, representative for any given rotorcraft configuration. Thus, the fuselage can be considered as a major design driver concerning weight, offering high weight saving potential.

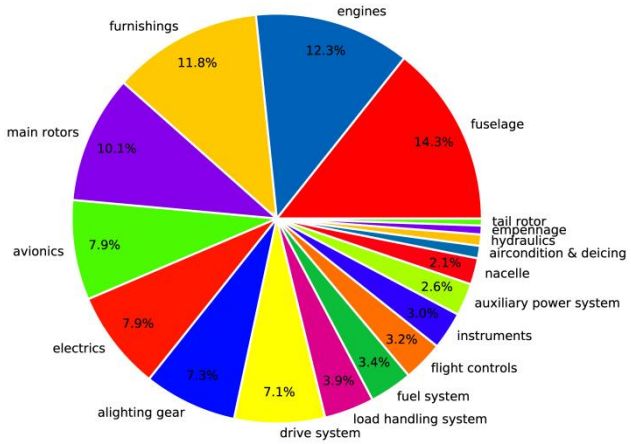

FIGURE 8. Composition of m_{em} (calibrated AFDD models)

Comparing the aforementioned methods to estimate rotorcraft component weights it can be observed that the body surface s_b constitutes an important parameter for the estimation of certain components.

Beltramo and Morris use one regression formula for the fuselage mass m_{fus} which is a function merely of the body surface s_b (see Eq. 6). They do not differentiate between different weight classes or rotorcraft types:

(6) $$m_{fus} = f(s_b)$$

Like Beltramo and Morris, Layton's fuselage mass estimation depends solely on the body surface. However, Layton classifies three different weight types of helicopter (see Tab. 1) and provides a formula for each.

Weight class	**m_{mto} range [lb]**
Light	m_{mto} < 3,000 (≈ 1,360.78 kg)
Medium	3,000 ≤ m_{mto} ≤ 25,000 (≈ 11,339.82 kg)
Heavy	m_{mto} > 25,000

TAB 1. Weight classes according to Layton

The approach of Palasis in general can be seen as a mixture of the formulas provided by Beltramo and Layton and therefore, it will not be described in detail within this paper.

The earlier methods, represented by Beltramo and Morris, and Layton that solely depend on the body surface are shown in Fig. 9.

As mentioned earlier, Layton groups rotorcraft in three different weight classes depending on their m_{mto}. It can be observed from Fig. 9 that the use of his *light rotorcraft* - formula would lead to an excessive estimation of the fuselage mass for increasing body surface. Note, that the formula for heavy helicopters has not been included in the diagram due to clarity reasons since it is not applicable in the presented body surface range.

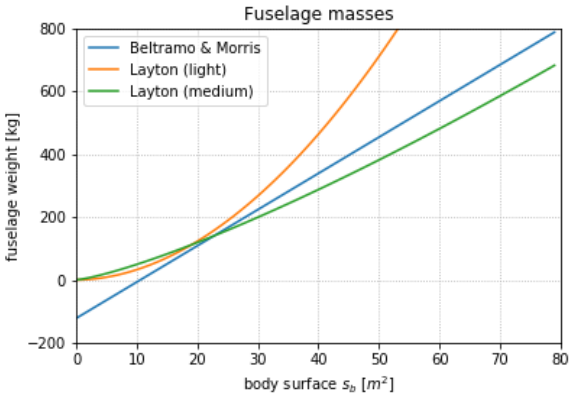

FIGURE 9. Fuselage mass calculation (Beltramo and Morris, and Layton) as function of body surface

As mentioned above, the body surface s_b does represent an important parameter for the weight estimation process since it coarsely overviews the size, thus the overall weight of the rotorcraft. Within IRIS it can be calculated by two possibilities:

- TIGL functions, or
- Approximations provided by Layton.

The weight estimation module supports both methods. However, instabilities could be observed for the body surface calculation with TIGL functions. Therefore, the surface calculation follows the *try-except-rule*: If the TIGL calculation does not succeed, the approximation formulas by Layton are applied. These functions are provided for three different weight classes of helicopter:

(7) $$s_{b,light} = 194.274 \cdot \ln(W_e) - 1306.779$$

(8) $$s_{b,medium} = 636.081 \cdot e^{0.0000098 \cdot W_g}$$

(9) $$s_{b,heavy} = 426.378 \cdot e^{0.000045 \cdot W_g}$$

with

W_e empty weight (in lb, corresponds to m_{em}),

W_g design gross weight (in lb, corresponds to m_{mto}).

Considering the fuselage weight estimations provided by Beltramo and Morris it is observable that for very small rotorcraft (s_b < ~10 m^2) the use of their method might lead to negative fuselage masses. This must be taken into account when being applied to very small rotorcraft representing urban mobility concepts, similar to e.g. the

Volocopter [20] or Ehang 184 [21] that are shown below in Fig. 10 and Fig. 11.

FIGURE 10. Volocopter [20]

FIGURE 11. Ehang 184 [21]

Taking the cockpit (respectively fuselage) dimensions as specified by Volocopter [20] and Ehang [21], and assuming a cuboid shape which leads to a conservative body surface (i.e. the real body surface is less than assumed), results in the estimated fuselage masses as shown in Tab. 2. Assuming surface correction factors of f = 0.8 and f = 0.9 to account for the deviation of the presumed cuboid shape to the real shape (for instance with regard to the inclined aerodynamic front resp. windshield), the fuselage mass can turn negative for the Ehang 184, highlighting the sensitivity of applying these methods to urban mobility concepts. Therefore, the aforementioned methods shall be applied with caution to prevent defective weight estimations for rotorcraft configurations other than the typical ones, as shown in Fig. 1.

Rotorcraft	**l [m]**	**w [m]**	**h [m]**	**s_b [m²]**	**m [kg]**
Volocopter	3.20	1.25	1.21	18.77	93.87
Volocopter (f=0.9)				16.89	72.28
Volocopter (f=0.8)				15.02	50.69
Ehang 184	2.07	1.02	1.45	13.17	29.5
Ehang 184 (f=0.9)				11.85	14.33
Ehang 184 (f=0.8)				10.54	-0.82

TAB 2. Dimensions and estimated fuselage masses (Beltramo and Morris) for urban mobility concepts (values rounded)

It shall also be noted that, at the time Beltramo and, Morris and Layton published their methods, the use of composite materials was comparatively rare so that the presented methods are mainly based on metallic structures. A calibration of the methods with respect to composite material has not been performed yet.

Constituting an enhancement for the weight estimation of rotorcraft fuselages, Prouty and Johnson reduced the dependence on the body surface by increasing the parameter range for the fuselage mass on additional factors, as shown in Eq. 10 and 11:

$$(10)\ m_{fus} = f\left(m_{mto}, l_{fus}, s_b\right)$$

Like Beltramo and Morris, Prouty and Johnson only provide one general method for the fuselage mass estimation for all rotorcraft weight classes.

The AFDD model 82, as provided by Johnson, introduces additional dependencies:

$$(11)\ m_{fus} = f(\chi_{fus}, f_{ramp}, m_{mto}, n_z, s_b, l_{fus})$$

where

χ_{fus} technology factor for the fuselage,

f_{ramp} factor for consideration of a cargo ramp,

n_z design ultimate flight load factor.

Additionally to the body surface, Prouty and Johnson take the fuselage length and the maximum take-off weight into account. Thus, they introduce a dependence on the geometric shape and overall weight. The inclusion of the maximum take-off weight can be seen as a first step towards an overall consideration of the rotorcraft: As mentioned earlier in Eq. 3 - 5, m_{mto} is partly the sum of the group masses which in turn are the sums of the corresponding masses of the components that are integrated into the helicopter. Depending on the required field of application of the helicopter, certain mission equipment is not considered during the design, e.g. civil transport helicopters do not need ballistic protection while avionics on military helicopters may include electronic countermeasures and identification friend or foe systems. Optical and infrared cameras, dunking sonar and search radars for anti-submarine helicopters will likely not be installed on civil helicopters. These operational items may strongly influence the design gross weight, even when the geometric properties are the same for two different rotorcraft configurations.

Taking a closer look on the methods provided by Prouty (Eq. 12)

$$(12)\ m_{fus} = 6.9 \cdot \left(\frac{m_{mto}}{1{,}000}\right)^{0.49} \cdot l_{fus}^{0.61} \cdot s_b^{0.25}$$

and Johnson (Eq. 13)

$$(13)\ m_{fus} = \chi_{fus} \cdot 5.896 \cdot f_{ramp} \cdot n_z^{0.1323} \cdot l_{fus}^{0.61} \cdot \left(\frac{m_{mto}}{1{,}000}\right)^{0.4908} \cdot s_b^{0.2544}$$

one can see that Johnson's method for the fuselage mass is very similar to Prouty's (neglecting minor deviations for two exponents, namely s_b and $m_{mto}/1000$), except that Johnson utilizes additional scaling factors. Besides the factor that accounts for a cargo ramp installation, Johnson considers the ultimate design flight load factor. With this approach Johnson considers the expected operational use of the helicopter, i.e. mission requirements respectively flight maneuvers which strongly influence the structural design. As an example, a utility or transport helicopter

(UTH) of (approximately) the same (geometric) size and/or design gross weight can be expected to experience less severe maneuvers. In contrast, a combat helicopter is supposed to conduct more challenging maneuvers than the UTH, e.g. narrow turns or hard pitch downs. Therefore, the military helicopter is expected to experience higher load factors, so the structural demand is higher which in turn requires a stiffer airframe potentially resulting in a higher structural mass.

Figure 12 shows a comparison of Prouty's and Johnson's method for the fuselage mass estimation as a function of the body surface s_b and the fuselage length l_{fus}. It can be observed that Johnson's method (illustrated by the spectral color map) corresponds to the one provided by Prouty (illustrated as blue surface) with an offset which is caused by the additional scaling parameters. It is also observable, that a bigger helicopter (i.e. s_b and/or l_{fus} increase) entails a mass increase.

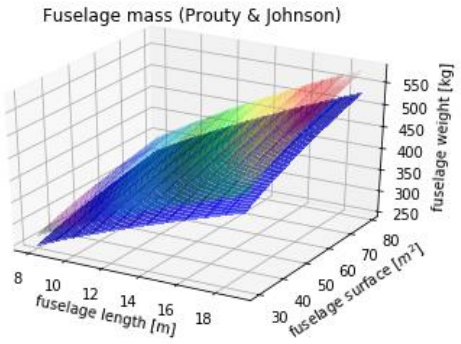

FIGURE 12. Fuselage mass calculation (Prouty and Johnson) as function of body surface and fuselage length

Table 3 shows the calculated fuselage masses applying Prouty's and Johnson's method to the aforementioned urban mobility concepts, assuming

f_{ramp} = 1.0,

n_z = 2.5, and

χ_{fus} = 1.0

for Johnson's method.

Rotorcraft	**m_{mto} [kg]**	**Prouty [kg]**	**Johnson [kg]**
Volocopter	450	49.33	48.70
Volocopter (f=0.9)		48.04	47.42
Volocopter (f=0.8)		46.65	46.02
Ehang 184	360	31.06	30.62
Ehang 184 (f=0.9)		30.26	29.81
Ehang 184 (f=0.8)		29.38	28.93

TAB 3. Dimensions and estimated fuselage masses (Prouty and Johnson) for urban mobility concepts (values rounded)

It can be seen, that the methods of Prouty and Johnson calculate a much lighter fuselage. Moreover, it can be observed that the application of surface correction factors do not severely influence the estimated weight, indicating a stable weight estimation. It shall be mentioned, that applying technology factors to account for advanced technologies, e.g. new materials, may further reduce the estimated weight. However, it shall be taken into account that all empirical models mentioned above were derived with respect to a fuselage comparable to the assembly shown in Fig. 5. A calibration of these models with a more sophisticated analysis performed in the preliminary design stage can minimize these uncertainties.

The estimation of the component weights is not only important for the calculation of an updated m_{mto} in the context of the conceptual sizing loop but also for the mass distribution for subsequent analysis with higher fidelity tools, e.g. in the preliminary design stage as described in ch. 5.

5. COMPUTATIONAL WEIGHT ASSESSMENT

As already mentioned, the conceptual design approach to estimate the fuselage weight depends on statistics and gives only a rough estimate. It often does not take into account specific performance requirements like flight maneuvers, or specific configurations, such as compound configurations that feature additional lifting surfaces.

Due to the continuously increasing computational power nowadays, a finite element (FE) analysis module was integrated into IRIS. This tool requires more input, quantitatively and qualitatively seen, than the conceptual design tools mentioned above. The computational time and the time required for the processing of input and output are also higher. Therefore, it is considered as L2 tool, representing preliminary design stage.

Subsequently the model generation, the analysis, and an implemented sizing routine for static and quasi-static load cases will be introduced.

5.1. Model generation

At the end of the conceptual design stage the outer fuselage shape, i.e. the loft, has been determined. To continue with a structural FE analysis, the stiffness distribution must be known. Therefore, as a first step in the preliminary design phase, the primary structure is defined within the prescribed loft. Knowledge based design criteria are used to distribute skin reinforcements such as frames and stringers, e.g. cutouts must be reinforced. In addition, hard points that are used for the integration of key components, such as the rotors, gear box, and alighting gear, or other heavy components, must be attached to reinforced structure. Figure 13 shows the applied scheme (for visibility reasons the skin panels have been removed): The first step denotes the conceptual design phase, at the end of which an outer fuselage loft has been derived with the external configuration. Further requirements concerning cutouts and main frame positions have also been elaborated. Now – depending on the operational boundaries – the primary structure can be defined. The figure exemplary shows four different possible airframe configurations which are all based on the same rotorcraft loft. Each configuration will result in a different structural mass when analyzed respectively sized according to the excepted ground- and flight load cases.

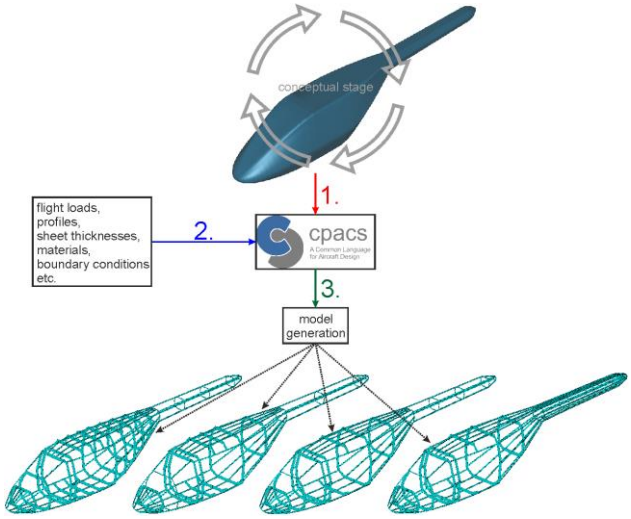

FIGURE 13. FE model preparation

Currently APDL (ANSYS Parametric Design Language) is used for the model generation allowing parametric modeling and automated execution.

The airframe is modeled using an approach as introduced by Hunter [22]: Stringers are discretized using elastic beam elements (BEAM188) that offer provision with arbitrary cross sections which allows the direct transfer of the profile data as described in the CPACS file. Applying the */ESHAPE* command in ANSYS allows a visualization of the provided cross section(s). Frames are discretized as extruded profiles using elastic shell elements (SHELL181). Along their edges beam elements (BEAM188) can be applied to account for any flanges, as shown in Fig. 14.

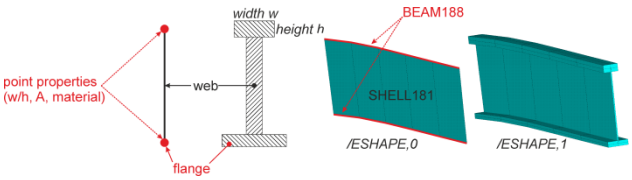

FIGURE 14. Mixed frame discretization

By default, the mesh is of global mesh quality (GFEM) which means that each bay (that is defined by two adjacent stringers and frames) forms one shell element representing the skin panels. An algorithm analyzes the frames and stringers and calculates their intersections. At each intersection an interpolation point is generated that serves as node in the following model generation. Moreover, the GFEM approach does not feature joint element modeling, e.g. cleats that connect frames and stringers to each other as well as to the skin panels. This additional weight increase is taken into account with an additional weight factor, scaled to the fuselage mass. Shanley [23], for instance, numeralizes the weight increase due to joints in the range of 20 % - 40% of the ideal minimum weight for metallic structures.

An FE model of a generic light utility helicopter airframe with cutouts for the windshield and doors is shown in Fig. 15.

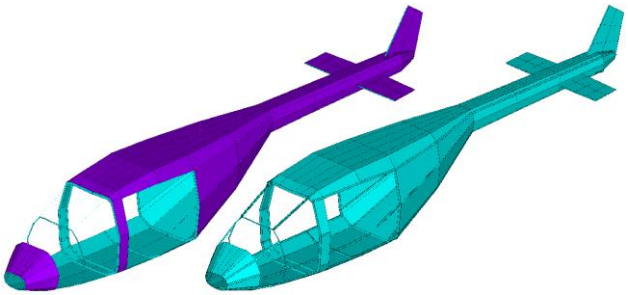

FIGURE 15. FE model (left side */ESHAPE,0* and right side */ESHAPE,1*)

So-called structural elements (consisting of profiles and material properties) are extruded either in longitudinal (stringers) or circumferential (frames) direction. Considering the stringers this approach would lead to an unreasonable stiffness and weight increase of the tail boom. Therefore, a virtual dummy structural element type *none* was implemented in the model generation. Dividing a structural member, i.e. stringer or frame, into several stages allows applying different structural elements to one structural member. This approach is called *stage modeling* and allows the provision with the virtual dummy element. This method is used to virtually reduce the stringers of the tail boom representing a realistic stiffness distribution and weight for the tail (see Fig. 16). Moreover, stage modeling is used to describe cutouts for passenger or cargo doors.

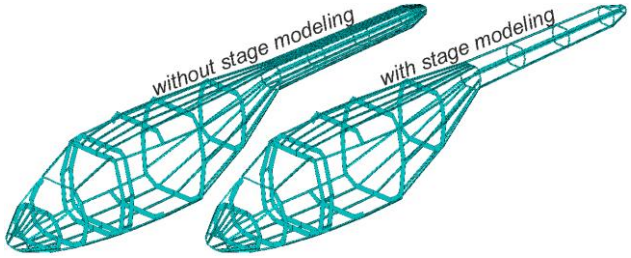

FIGURE 16. Stage modeling applied to the tail boom

As indicated earlier do the interpolation points determine the airframe structure. The more interpolation points are available the better the fuselage loft can be represented. Therefore, virtual dummy elements can be used to artificially increase the amount of interpolation points and, thus, to generate a geometrically more realistic airframe. Figure 17 shows an exemplary airframe with only four stringers. On the left a comparably coarse geometry is shown while the model on the right shows the same airframe with additional stringers featuring the virtual dummy elements at the top and bottom side of the fuselage. Therefore, the model on the right features more interpolation points. It can be seen that this model features a smoother bottom and top surface representing the fuselage loft more precisely while the model on the left strictly connects both lower and upper stringers, respectively, with straight elements.

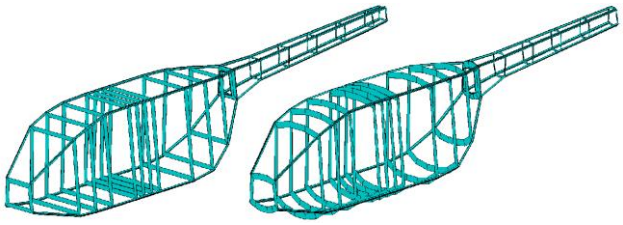

FIGURE 17. Influence of the amount of interpolation points on the model accuracy

More details on the modeling approach and on specific options, such as the structural element type *none*, cutouts, and stage modeling are given by Schwinn [24].

The component masses that have been estimated during the conceptual design phase are modeled as lumped masses at additional nodal points. They are constrained to the airframe over a user-specified region, as exemplary shown in Fig. 18.

External forces and moments generated at the rotors are applied at the corresponding nodes and constrained to a user-specified region of the airframe. Figure 18 exemplary shows the airframe (without skin panels for visibility reasons) and two nodal masses representing the main and tail rotor. At each node the acting force is displayed by the red arrow while the constraints that introduce the load into the airframe are shown in magenta. This modeling approach conditions that external forces (and moments) can only be applied at nodes representing nodal masses. Gravity is modeled as an acceleration field acting on all structural nodes and elements.

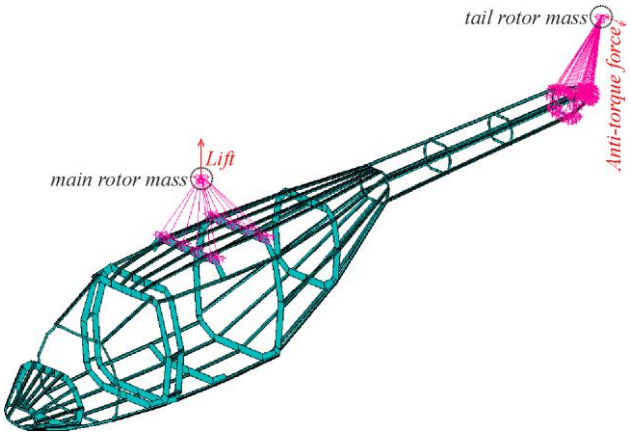

FIGURE 18. Force and mass constraints

The model is fixed in space at a node close to the computed center of gravity (COG). Potentially remaining forces due to little load inconsistencies during trim are compensated using the inertia relief option. This approach allows the calculation of stresses and strains without dynamic analyses by introducing artificial boundary conditions for equilibrium of forces and moments.

The loads calculation uses the fuselage weight which has been estimated during the conceptual design phase for the calculation of the required lift forces. A more detailed description of the loads calculation process as it is currently implemented is given by Schwinn et al. [25].

To conclude the model generation section it shall be noted that currently only isotropic materials are implemented for the computational analysis. However, it is intended to integrate orthotropic materials into the analysis process during the TRIAD project.

Depending on a user-specific entry in the CPACS file it is possible to either merely generate an FE model, to conduct a static analysis of a chosen load case (see ch. 5.2), or to conduct a sizing process (see ch. 5.3).

5.2. Static analysis

Static analyses are conducted using the linear-elastic solver in ANSYS. Exemplary, a hovering analysis of a generic utility rotorcraft with cutouts for the pilot doors (2x), cabin doors (2x) and for the windshield is shown in Fig. 19: The left figure displays the airframe while – for visibility reasons – the skin panels have been removed in the center graph. The right graph shows the frames only. The fuselage structure is made of aluminum 2024 with flat frames of different heights. The thicknesses of the frames vary between $1.4 \leq t \leq 1.6$ [mm] while the skin panels feature a thickness of $t = 1.0$ [mm] and the hat shaped stringers feature sheet thicknesses of $t = 1.4$ [mm]. The material properties are displayed in Tab. 4.

Young's modulus [GPa]	67.7
Density ρ [kg/m^3]	2,800
Poisson's ration [-]	0.248
Yield strength [MPa]	320

TAB 4. Aluminum 2024 – material properties

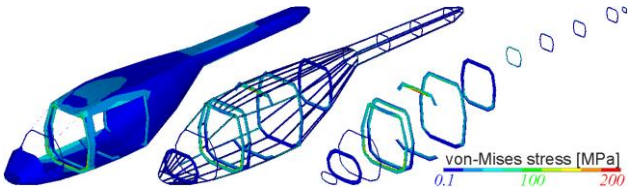

FIGURE 19. Static hovering analysis (coarse discretization)

It can be observed from Fig. 19 that the highest stresses arise where the heaviest masses are located and the external loads from the rotors are introduced. It can also be seen that due to the fuselage cutouts the load is transferred around the cutout in the adjacent frames while the highest stress is located in the center frame of the cutout where the main rotor is located. Additionally, it can be observed that the lateral force generated by the tail rotor (to compensate the torque of the main rotor) leads to a stress increase at the transition frame between fuselage cabin and tail boom. The tail boom can be considered as a beam under bending load clamped at the aforementioned transition frame.

Applying a finer discretization in detailed FEM (DFEM) quality to the same model, as shown in Fig. 20, a mesh dependent behavior can be observed.

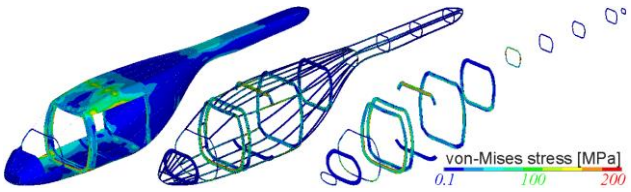

FIGURE 20. Static hovering analysis (fine discretization)

This dependence is substantiated that the mesh is not fine enough to calculate local stress peaks, so the stresses are averaged over the larger areas, i.e. the larger element sizes. Therefore, localized stress concentrations cannot be adequately shown with the coarse GFEM approach.

However, it shall be noted that for preliminary purposes, the GFEM approach is considered as sufficient because of the faster pre- and post-processing, faster computations, and smaller file sizes in relation to the required level of detail.

5.3. Sizing approach

Structural sizing is conducted using an APDL based sizing module. It was originally developed for sizing of aircraft wings [26] and enhanced to size transport aircraft fuselages [27]. During the EDEN project it was extended for the use of rotorcraft fuselages [28].

Strength evaluation is based on fully stressed design (FSD) principles. To guarantee sufficient safety against stability failure, local compressive and shear buckling methods as provided by Bruhn [29] have been implemented.

For each element the equivalent stress σ_{eqv} is computed. This stress value is then used to individually size the element with a scaling factor according to

$$(14)\ sf = \frac{\sigma_{eqv,max,a}}{\sigma_{eqv}}$$

where $\sigma_{eqv,max,a}$ describes the maximum allowable equivalent stress, as specified by the material or stability limits (in the CPACS file).

Shell elements are sized by their thickness. Beam elements are sized by a common scale factor for their individual sheet thicknesses.

This process is repeated for each specified load case and the maximum required element thickness respectively sheet thicknesses are stored. The stress states in all elements are then recalculated with the updated stiffness distribution until convergence is achieved, as schematically illustrated in Fig. 21. The final thicknesses and cross sections are saved in the CPACS file as well as the updated mass breakdown due to the new values for m_{struct}, m_{oem}, and m_{mto}.

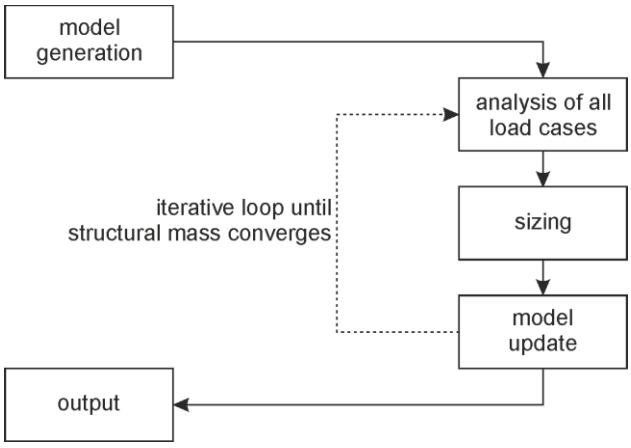

FIGURE 21. Flowchart of the structural sizing module

This step allows feedback to the conceptual design loop to allow a resizing of the external configuration with respect to special performance requirements affecting the structural design.

An exemplary sizing process for a light utility helicopter, as illustrated in Fig. 18 - 20, is displayed in Fig. 22. The load cases that were used for the sizing are listed below in Tab. 5.

Model number	Load case (added)
01	hovering
02	01 + maximum cruise
03	02 + jump take-off
04	03 + turns
05	04 + 2.5g pull

TAB 5. Load case description

Figure 22 shows the mass development (logarithmic) over iterations with increasing number of considered load cases converging in general after five to six iterations. It can be seen, that the weight increases due to the addition of new load cases with the 2.5g pull maneuver evoking the highest weight. However, it must be noted that the sole calculation of the 2.5g pull cannot be seen sufficient for the structural sizing since several load cases call responsible for different areas of the airframe.

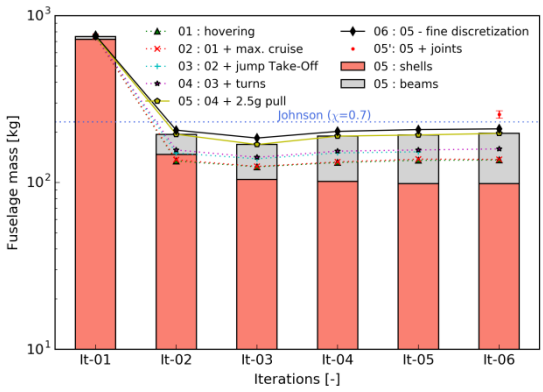

FIGURE 22. Sizing process for an UTH

Model 06 corresponds to model 05, except that the finer discretization approach has been chosen (see Tab. 6).

Model	Nodes[2]	Shells	Beams	Time [s]
05 (coarse)	650	480	100	156
06 (fine)	8,830	7,250	960	638

TAB 6. Discretization approaches (rounded values)

The weight estimated using the calibrated AFDD models is represented by the dashed line. The red marker in the converged iteration number six (It-06) with the error bars represents the additional weight range of the joints (applied to model 05) as proposed by Shanley indicating good agreement of the statistical and the numerical approach at this early design stage. The stringer sizing allowed a wide range, potentially scaling the sheet thicknesses t of each stringer S_i in a range of

[2] Including orientation nodes for beam elements

(15) $0.5 \cdot t_{Si,original} \leq t_{Si,new} \leq 5.0 \cdot t_{Si,original}$

Comparing model 05 and model 06 to each other it can be noted that the finer discretization results in a slightly higher weight – caused by the increased amount of nodes and elements that represent the geometry more accurate compared to the coarse model. However, it must be noted that the increase in computational time to conduct the sizing process exceeds the acceptable time regarding preliminary design level.

Figures 23 and 24 show the resulting thickness distribution for the shell elements (representing the frames and the skin panels) for the coarse and fine discretization. As seen at the static computation, the stresses in the coarse computation are averaged over a larger area so that the required thicknesses are comparably less. In contrast, the finer discretization shows higher required local thicknesses for some critical areas, such as the frame between the cutouts for the doors or the frame where the main rotor is attached to.

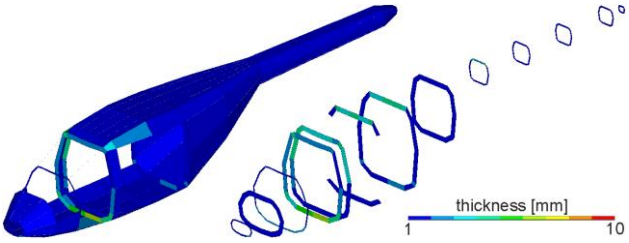

FIGURE 23. Model 05: Thickness distribution

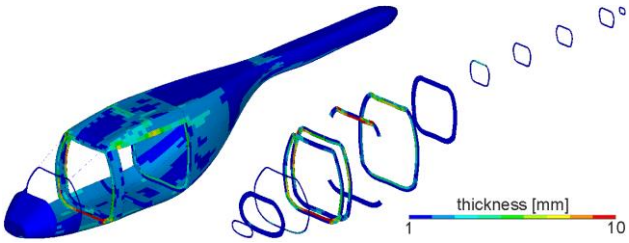

FIGURE 24. Model 06: Thickness distribution

As mentioned above, the airframe is sized due to the influence of different load cases at different areas. Figure 25 overviews the airframe and its dependence on the specified load case. The numbers that are specified in the legend refer to the number depicting the individual load case as given in Tab. 5 and Fig. 22 (with 3a and 3b representing different turns).

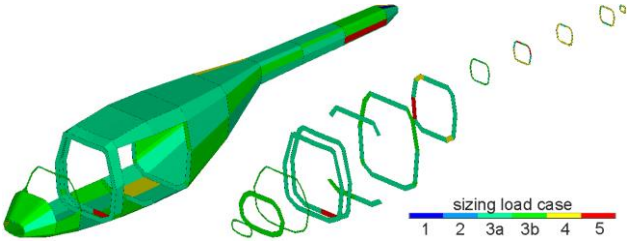

FIGURE 25. Model 05: Critical load cases

Figure 26 shows the relevant sizing criteria for the shell elements. It can be observed that most of the elements are sized either according to strength limits (maximum von Mises stress), shell bucking criteria, and the minimum thickness criteria. The minimum thickness criterion is applied since the surrounding stringers take a significant share of the load.

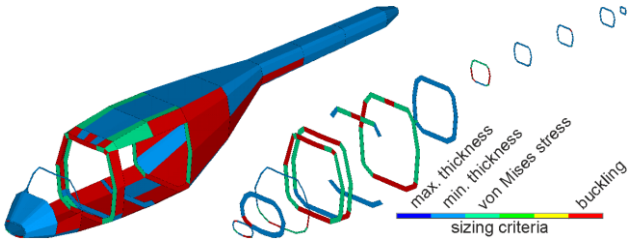

FIGURE 26. Model 05: Sizing criteria

Figure 27 visualizes the stringer sizing using different colors. The original model before sizing had an identical stringer distribution, i.e. all stringers had the same cross section and material properties.

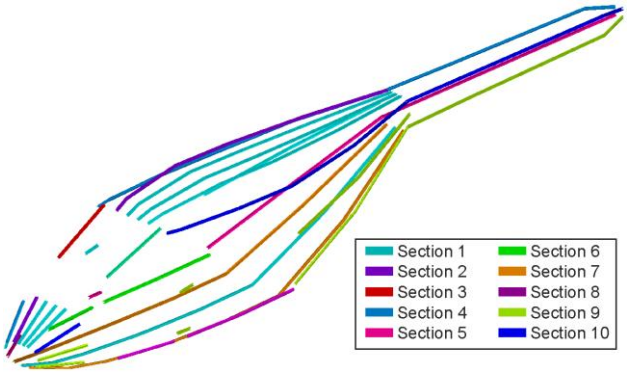

FIGURE 27. Model 05: Stringer sizing

Section 1 (S_1) represents the original stringer profile, as depicted in Fig. 28.

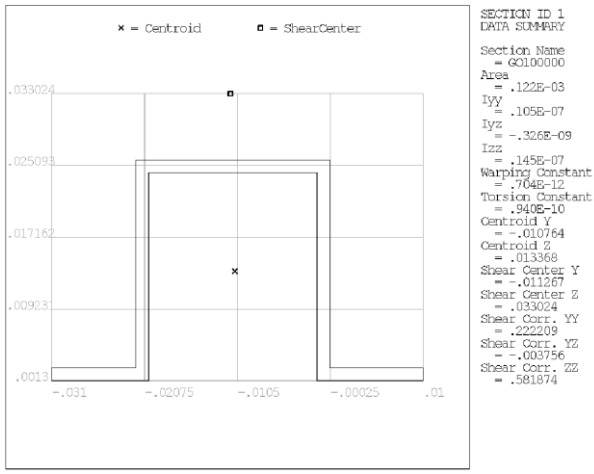

FIGURE 28. Model 05: Stringer geometry (section 1)

Exemplary, section 2 (S_2) is illustrated in Fig. 29. As mentioned above, beam elements are sized by equally scaling their sheet thicknesses. The sheet thicknesses of section 2 correspond to

(16) $t_{S2} = 2.2 \cdot t_{S1}$

It can be seen that section 2 shows similar but scaled sheet thicknesses compared to the shape of the original omega-hat-shaped geometry S_1.

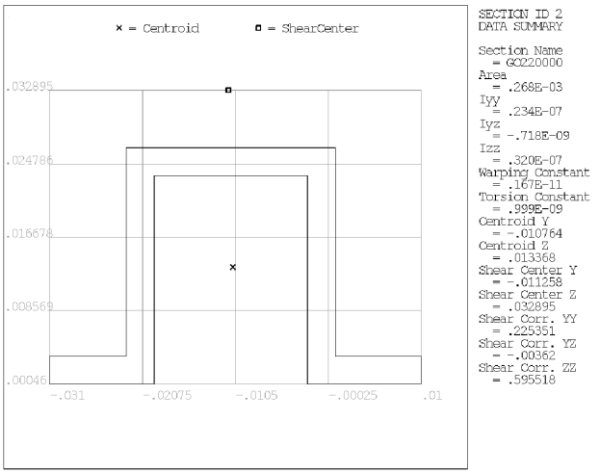

FIGURE 29. Model 05: Stringer geometry (section 2)

6. CONCLUSION AND OUTLOOK

The presented paper introduced the design environment IRIS with particular focus on the weight assessment. Methods to estimate the mass breakdown of a rotorcraft configuration were presented for the conceptual design and preliminary design stages. The approaches to estimate the fuselage weight were explained in detail and their ad- and disadvantages were highlighted.

In order to profit at early design stages from the steadily increasing numerical power, an approach to numerically size the fuselage to calculate its structural mass was introduced. Exemplary analyses and sizing processes were shown.

To further enhance the presented weight estimation methods, future enhancements during the TRIAD project comprise:

- The integration of composite materials will allow tailoring of the material according to the load paths, thus promising significant weight saving potential.
- In order to reduce the dependence on commercial FE solvers and therefore license availability and costs, the presented FE module will be reconstructed and integrated into the solver independent framework software PANDORA (Parametric Numerical Design and Optimization Routines for Aircraft, [30]) which is currently under development at the DLR Institute of Structures and Design.
- The loads calculation process will be transferred to HOST to integrate more flight maneuvers and therefore load cases into the sizing process.
- A more detailed, and therefore, more realistic mass distribution that dispenses with nodal point masses, is required to improve the static analysis and sizing routines. Moreover, a more detailed mass distribution may allow an extension of the considered load cases and also additional dynamic assessment of the fuselage.

7. ACKNOWLEDGEMENTS

The work presented in this manuscript has been achieved within the DLR projects EDEN (Evaluation and Design of Novel Rotorcraft Concepts), FAST-Rescue (Fast and Silent Rescue Helicopter), and TRIAD (Technologies for Rotorcraft in Integrated and Advanced Design). The authors would like to gratefully acknowledge and appreciate the financial support. Additionally, the authors would like to express their gratitude to Dieter Kohlgrüber, Joachim Götz, Jonas Jepsen, Arthur Zamfir, Thomas Weber, and Christian Haschert for their valuable contribution to TRIAD and the fruitful discussions.

This conference article is a preprint of an article published in the CEAS Aeronautical Journal. The final peer-reviewed version of this article has been published open-access (CC BY 4.0) and is available online at http://link.springer.com/article/10.1007/s13272-021-00492-z.

8. REFERENCES

[1] D. P. Raymer. *Aircraft Design: A Conceptual Approach*. American Institute of Aeronautics and Astronautics (AIAA) Education Series, 1992.

[2] B. Nagel, D. Böhnke, V. Gollnick, P. Schmollgruber, A. Rizzi, G. La Rocca and J. J. Alonso. Communication in Aircraft Design: Can We Establish a Common Language?. In *28th International Congress of the Aeronautical Sciences*, Brisbane, Australia, 2012.

[3] D. Seider, M. Litz, A. Schreiber and A. Gerndt. Open Source Software Framework for Applications in Aeronautics and Space. In *IEEE Aerospace Conference*, Big Sky, MT, USA, 2012.

[4] TIXI homepage. *https://github.com/DLR-SC/tixi.* [accessed August, 28th 2018]

[5] TIGL homepage. *https://github.com/DLR-SC/tigl.* [accessed August, 28th 2018]

[6] P. Weiand, D. B. Schwinn, M. Schmid and M. Buchwald. A Multidisciplinary Process for Integrated Rotorcraft Design. In *43rd European Rotorcraft Forum*, Milan, Italy, 2017.

[7] A. Krenik and P. Weiand. Aspects on Conceptual and Preliminary Helicopter Design. In *Deutscher Luft- und Raumfahrtkongress (DLRK)*, Braunschweig, Germany, 2016.

[8] P. Kunze. Parametric Fuselage Geometry Generation and Aerodynamic Performance Prediction in Preliminary Rotorcraft Design. In *39th European Rotorcraft Forum*, Moscow, Russia, 2013.

[9] B. Benoit, A.-M. Dequin, K. Kampa, W. Grünhagen, P.-M. Basset and B. Gimonet. HOST, a General Helicopter Simulation Tool for Germany and France. In *American Helicopter Society 56th Annual Forum*, Virginia Beach, VA, USA, 2000.

[10] M. Buchwald, P. Weiand, D. B. Schwinn and M. Schmid. Flight performance calculation of rotorcraft in the conceptual design phase. In *Deutscher Luft- und Raumfahrtkongress (DLRK)*, Friedrichshafen, Germany, 2018.

[11] P. Weiand, M. Schmid, M. Buchwald and D. Schwinn. A distributed design environment for rotorcraft. In *Deutscher Luft- und Raumfahrt Kongress (DLRK)*, Friedrichshafen, Germany, 2018.

[12] E. Torenbeek. *Advanced Aircraft Design*. John Wiley & Sons, Ltd., 2013.

[13] Society of Allied Weight Engineers. SAWE RP No. 8A - Weight and Balance Data Reporting Forms for Aircraft (including Rotorcraft and Air-Breathing Unmanned Aerial Vehicles) - Revision 1. 1997.

[14] M. N. Beltramo and M. A. Morris. Parametric study of helicopter aircraft systems costs and weights. NASA-CR-152315, 1980.

[15] D. M. Layton. *Introduction to Helicopter Conceptual Design (Home Study Correspondence Course).* American Institute of Aeronautics and Astronautics (AIAA) Professional Studies Series, Sep.1991 – Mar.1992.

[16] D. Palasis. *Erstellung eines Vorentwurfsverfahrens für Hubschrauber mit einer Erweiterung für das Kipprotorflugzeug*. Phd thesis, Universität der Bundeswehr, Munich, Germany, 1992.

[17] R. W. Prouty. *Helicopter Performance, Stability, and Control*. Krieger Publishing Company, 2002.

[18] W. Johnson. NDARC - NASA Design and Analysis of Rotorcraft. NASA/TP–2009-215402, 2009.

[19] C. Russell and P.-M. Basset. Conceptual Design of Environmentally Friendly Rotorcraft - A Comparison of NASA and ONERA Approaches. In *American Helicopter Society 71th Annual Forum*, Virginia Beach, VA, USA, 2015.

[20] Volocopter homepage. *https://www.volocopter.com/de/product/,* 2018. [accessed July, 27th 2018].

[21] Ehang homepage. *http://www.ehang.com/ehang184/specs/,* 2018. [accessed August, 1st 2018]

[22] E. W. Hunter. A Process to Enable High Fidelity Airframe Sizing and Optimization for Conceptual Design. In *49th AIAA/ASME/ASCE/AHS/ASC Structures, Structural Dynamics, and Materials Conference*, Schaumburg, IL, USA, 2008.

[23] F. R. Shanley. *Weight-Strength Analysis Of Aircraft Structures*. Dover Publications, Inc., 1960.

[24] D. B. Schwinn. Applied parametrized and automated airframe modeling methods in the preliminary design phase. *International Journal of Modeling, Simulation, and Scientific Computing,* 6(4):1550037, 2015.

[25] D. B. Schwinn, P. Weiand, M. Schmid and M. Buchwald. Structural sizing of a rotorcraft fuselage using an integrated design approach. In *31th Congress of the International Council of the Aeronautical Sciences*, Belo Horizonte, MG, Brazil, 2018.

[26] B. Nagel, M. Kintscher and T. Streit. Active and Passive Structural Measures For Aeroelastic Winglet Design. In *26th International Congress of the Aeronautical Sciences*, Anchorage, AK, USA, 2008.

[27] J. Scherer, D. Kohlgrüber, F. Dorbath and M. Sorour. A Finite Element Based Tool Chain for Structural Sizing of Transport Aircraft in Preliminary Aircraft Design. In *Deutscher Luft- und Raumfahrtkongress (DLRK)*, Stuttgart, Germany, 2013.

[28] D. B. Schwinn, P. Weiand and M. Schmid. Structural Analysis of a Rotorcraft Fuselage in a Multidisciplinary Environment. In *NAFEMS World Congress*, Stockholm, Sweden, 2017.

[29] E. F. Bruhn. *Analysis and Design of Flight Vehicle Structures*. Tri-State Offset Company, 1973.

[30] M. Petsch, D. Kohlgrüber and J.-N. Walther. Development of a fully automated transport aircraft fuselage modelling and sizing tool using Python. In *Deutscher Luft- und Raumfahrtkongress (DLRK)*, Munich, Germany, 2017.

[31] C. M. Liersch and M. Hepperle. A distributed toolbox for multidisciplinary preliminary aircraft design. *CEAS Aeronautical Journal,* 2:57, 2011.